Journal Pre-proof

Ultrathin, transparent, and robust self-healing electronic skins for tactile and non-contact sensing

Ruiyuan Liu, Yue Lai, Shaoxin Li, Feng Wu, Jianming Shao, Di Liu, Xia Dong, Jie Wang, Zhong Lin Wang

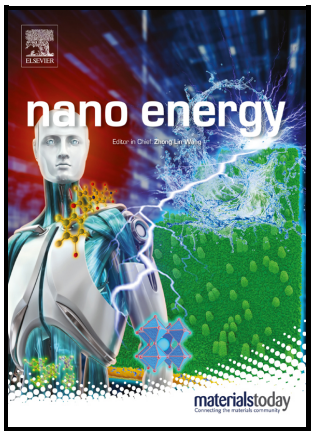

PII: S2211-2855(22)00140-9

DOI: https://doi.org/10.1016/j.nanoen.2022.107056

Reference: NANOEN107056

To appear in: *Nano Energy*

Received date: 17 December 2021
Revised date: 4 February 2022
Accepted date: 11 February 2022

Please cite this article as: Ruiyuan Liu, Yue Lai, Shaoxin Li, Feng Wu, Jianming Shao, Di Liu, Xia Dong, Jie Wang and Zhong Lin Wang, Ultrathin, transparent, and robust self-healing electronic skins for tactile and non-contact sensing, *Nano Energy,* (2021) doi:https://doi.org/10.1016/j.nanoen.2022.107056

Ultrathin, transparent, and robust self-healing electronic skins for tactile and non-contact sensing

Ruiyuan Liu[1,3#], Yue Lai[2,4,#], Shaoxin Li[1,4#], Feng Wu[5], Jianming Shao[2,4], Di Liu[1,4], Xia Dong[2,4]*, Jie Wang[1,4]*, Zhong Lin Wang[1,4,6]*

1. Beijing Institute of Nanoenergy and Nanosystems, Chinese Academy of Sciences, Beijing 100083, P. R. China.

2. CAS Key Laboratory of Engineering Plastics, CAS Research/Education Center for Excellence in Molecular Sciences, Institute of Chemistry, Chinese Academy of Sciences, Beijing 100190 P. R. China.

3. College of Energy, Soochow University, Suzhou 215006, P. R. China.

4. University of Chinese Academy of Sciences, Beijing 100049, P. R. China.

5. Research Institute of Information Technology, Tsinghua University, Beijing 100084, China.

6. School of Materials Science and Engineering, Georgia Institute of Technology, Atlanta Georgia 30332, United States.

[#]These authors contributed equally.

*E-mail: xiadong@iccas.ac.cn; wangjie@binn.cas.cn; zhong.wang@mse.gatech.edu.

ORCID:

Ruiyuan Liu: 0000-0002-1678-3500

Xia Dong: 0000-0002-6409-7011

Jie Wang: 0000-0003-4470-6171

Zhong Lin Wang: 0000-0002-5530-0380

Abstract

Thin, transparent, and robust self-healing electronic skins (e-skins) enable multifunction in wearable electronics, flexible displays and soft robotics. However, developing healable e-skins that can simultaneously attain sufficient flexibility, high transparency and stable operation is still a challenge. Here, we report an ultrathin, highly transparent and robust self-healing e-skin by introducing an

amorphous microphase-separated elastomer, with self-powered tactile and non-contact sensing functions. The 3-μm-thick e-skin exhibits a reduction of two orders of magnitude in thickness compared with previous self-healing devices, while exhibiting a high transparency of over 92% in visible wavelength. The excellent conformability of the e-skin enables seamless attachment onto human skin and generation of electrical signals for energy harvesting and active sensing based on the coupling effect of contact electrification and electrostatic induction. Moreover, the ultrathin e-skin is extremely robust, maintaining the identical electrical output performance after 45,000 bending tests and over 146,000 operational cycles. We finally demonstrate the non-contact control of a smart phone with this multifunctional e-skin as self-powered active sensor, providing a unique future for human-machine interactions.

Keywords

flexible electronics, self-healing, ultrathin, electronic skins, triboelectric nanogenerators

Introduction

Flexible electronic skins (e-skins) with conformable, transparent and self-healable features enable multifunctional applications in wearable devices, soft robotics and human-machine interfaces[1-5]. Conformability has been introduced to thin-film electronics by greatly reducing the device thickness, which enables superior deformation on the targeted surfaces without restriction of the movements and deterioration of performance. Examples include epidermal electronics, ultrathin films and nanomesh structures that could be directly laminated on to the surface of

the skin with thickness of a few micrometers[6-8]. Transparency provides visual transmission of information that is indispensable for optoelectronics such as electroluminescent devices, biomedical imaging and displays[9, 10]. Self-healing ability allows an e-skin to recover its critical functionality after mechanical damage, like human skin, guaranteeing highly sustainable and durable operations[3, 11-13]. Next-generation robust electronics with such synthetic features are multifunctional or even smart, offering new opportunities in a diverse range of research fields and real-world settings, such as energy, sensing and healthcare.

Very recently, advances have been made in healable soft electronics by creating conductive pathways in dielectric hydrogel or polymer matrix. Repeatedly self-healing devices with considerable electrical performance, mechanical flexibility, biocompatibility, and transparency have been successfully demonstrated, including optoeletronics[10], sensors[14], e-skins[15, 16] and energy devices[17, 18]. However, it is still challenging to develop efficient healable soft electronics that can simultaneously attain sufficiently low thickness with high flexibility, high transparency and stable operation. Most of the reported devices require a mold to encapsulate the liquid ionic conductor or hydrogel from leakage, which results in large device thickness (500 μm to several millimetres) and encapsulation problems under mechanical operation; some of the self-healing materials are inherently opaque; others using opaque electrodes like silver flakes, liquid metal or carbon based conductive materials that will dramatically decrease the transmittance. Consequently, self-healing e-skins that are thin, transparent and robust to realize a multifunctional platform are yet to be developed. For instance, a self-healable silver nanowire/polymer matrix composite has been developed with autonomously healability and a device thickness of 500 μm, but nearly no transparency[19].

Here, we report an ultrathin (a few micrometers), highly transparent (>92%) and robust self-healing e-skin for tactile and non-contact sensing based on amorphous microphase-separated elastomers. Homogeneous control of the elastomer by locking soft dynamic bonds in stiff polymer matrix enables fast self-healing, nearly 100% transparency and excellent mechanical properties. Benefiting from the amorphous microphase-separated materials design, facile control of freestanding ultrathin e-skins with thickness down to a few micrometers is achieved by embedding transparent conductive polymers in the elastomers. The combination of ultrathin device configuration, high transparency, excellent self-healing property and high mechanical flexibility enables the elastomers to be multifunctional platforms in the design of conformable soft materials for applications in soft robotics, human-machine interface and wearable electronics. To highlight the potential applications of this ultrathin film, we demonstrate a conformable triboelectric device that generates voltages of up to 26 V with human body motion through coupling effect of contact electrification and electrostatic induction. The 3-μm-thick self-healing e-skin is extremely robust, maintaining its identical electrical output performance after 45,000 bending tests at a radius of 0.5 mm and over 146,000 operational cycles. For the first time, we realize non-contact control of a smart phone with this self-healing and transparent e-skin, which especially provides a unique future for smart human-machine interactions.

Experimental section

Materials. Polytetramethylene ether glycol (PTMEG 1000) was purchased from Invista. Hydrogenated 4,4’-methylenediphenyl diisocyanate (HMDI) was purchased from Coverstro. Bis(2-hydroxyethyl) disulfide (HEDS, tech. 90 %) was purchased from Alfa Aesar. The catalyst dibutyltin dilaurate (DBTDL, tech.

97.5 %), the solvent N, N-dimethylacetamide (DMAc) and 1,6-hexanediol (HDO) were purchased from J&K Chemical Ltd. PEDOT:PSS was purchased from Heraeus. Polystyrene nanospheres with a diameter of 360 nm (5 wt%) was purchased from Suzhou Nano Micro Technology Co., Ltd. Materials synthesis was based on our previous report[19]. For prepolymer, PTMEG was first heated at 120 °C under vacuum for 2 h until melted to remove the moisture and then reacted with two equivalents of HMDI in the presence of the catalyst (DBTDL). Next, HEDS as a chain extender and DMAc as the solvent were added to the system to complete the synthesis. In addition, a blank control sample was obtained by adding HDO to the prepolymer instead of HEDS.

Characterization. Tensile testing was carried out by a universal tensile machine. The specimens were cut into a small dumbbell shape with a thickness of approximately 0.5 to 0.8 mm. All the tensile tests were performed under the following conditions: a strain rate of 100 mm/min, a gauge length of 4 mm, room temperature (approximately 25 °C) and a humidity of 60 ± 3 %. The average of the results of five individual tensile tests was recorded for each sample. Differential scanning calorimetry (TA Q200) was used to characterize the film thermal properties and was performed from -150 °C to 180 °C at a 20 °C·min^{-1} heating rate under nitrogen flow. Thermogravimetric analysis experiments were performed on a PE8000 instrument at a linear heating rate of 20 °C·min^{-1} from 30 to 800 °C under air atmosphere. The first-stage degradation temperatures of the samples are approximately 300 °C. The surface morphologies of the samples on microsubstrates were measured by tapping-mode atomic force microscopy (AFM, Bruker multimode 8) using tapping MPP-rotated cantilevers with silicon probes (name: RTESP, order MPP-11120-10, 40 N/m, 300 kHz, rotated tip). To measure the topography and roughness of the copolymer layer, the amplitude set point was adjusted above 250 mV, and both the AFM height and phase images were

collected simultaneously. To evaluate the self-healing ability of the sample bars, specimens were completely cut in half in air. Then, the two pieces of the elastomer samples were manually merged and heated at 70 °C using an oven for a preset time (3 h, 6 h, 12 h, or 24 h). During the self-healing process, no external stress was applied to the interface. The healed samples were again subjected to tensile tests. The tensile test conditions were the same as those mentioned above. Polarized optical microscopy (POM) images of the self-healing process of the samples were obtained by an Olympus (BX51) optical microscope equipped with a Canon 40 D camera system. A Linkam (THMS600E) hot stage was used to control the temperature. Scratched (by one side blade) elastomer films were placed on a heating stage (Linkam) at 70 °C, and optical microscopy was used to monitor the self-healing process. Raman spectra (LabRAM HR Evolution) of the synthesized samples were recorded on a microscope using a laser excitation wavelength of 532 nm. The spectra were generally collected over a spectral range from 1600 to 50 cm^{-1}. The integration time was 20 s, and the accumulation number was 2. Transparency tests were carried out by a SHIMADZU UV-2600 ultraviolet spectrophotometer with an integrating sphere attachment. Spectra were generally collected over a spectral range from 520 nm to 580 nm, and the scanning speed was medium mode.

Device fabrication and measurement. A silicon wafer was treated by plasma for hydrophilic surface and elastomer solution was spin-coated onto the wafer subsequently with different speed. 1 wt% Triton and 5 wt% DMSO were added into PEDOT:PSS solution and heated at 115 °C for 30 min to enhance the conductivity as well as decrease the surface energy. The conducting polymer was further coated on the elastomer film and transferred into a vacuum oven for 30 min at 115 °C. A second layer of elastomer was coated onto the PEDOT:PSS/elastomer sample to finalize the sandwiched device structure. The elastomers were cured at

60 °C in the oven under vacuum for at least 5 h. Monolayer polystyrene nanospheres with a diameter of 360 nm were self-assembled on water surface by dipping a drop of the ethanol diluted dispersions (2.5 wt%) onto a plasma treated silicon wafer floating on water. The nanospheres were then loaded onto the elastomer through a lifting process, followed by a natural water evaporation process in the ambient[20, 21]. A linear motor (LinMot E1100) was used to provide the input of mechanical motions. The force applied by the motor was detected by a LabQuest Mini force gauge (Vernier). The electrical output parameters of the TENGs were collected by a programmable electrometer (Keithley 6514) and recorded by a software written in LabVIEW.

Results and discussion

Design of the highly transparent, robust and self-healing thermoplastic elastomers. The self-healing elastomers consists of homogeneously separated stiff and soft components in microphases (Figure 1a). Polytetramethylene ether glycol (PTMEG) was used as the stable and inert soft segments to construct a mechanically elastic matrix. Hydrogenated 4,4′-methylenediphenyl diisocyanate (HMDI) and aliphatic disulfide bis(2-hydroxyethyl) disulfide (HEDS) were used as the active stiff segment to conduct self-healing function through the dynamic aliphatic disulfide bonding interactions. The elastomer exhibits excellent mechanical properties below the glass transition temperature (T_g) with the dynamic bonds locked in the stiff segments by microphase separation controlling, which is a "stiff phase locking" design. The self-healing process could be activated upon heat stimuli at temperatures above the T_g, as a result of dynamic disulfide bond exchange and strong hydrogen bonding interactions between the interfaces of

physically contacted elastomers (Figure 1b). Previous self-healing polymers based on disulfide bond exchange reactions usually contain high amounts of aromatic sulfide compounds, which result in yellowish color and decreased transparency, to achieve a fast healing rate[18]. The combination of using the aliphatic disulfide compounds (below 8 wt%) and the alicyclic isocyanates with high steric hindrance in this work allows for neutral transparent materials. The irregular packing of the molecular chains and strong hydrogen bonding in the stiff segments induce an amorphous micro-phase separation in the elastomer, which is the origin of the high optical transparency and facile film fabrication. As shown in Figure 1c and Figure 1d, samples with different thicknesses from 3 to 100 μm are all exhibiting exceptional transmittance of over 99.5% in the visible wavelength range (400-800 nm), which is highly desirable for optical applications. The amorphous microphase separation of stiff segments and soft segments enables the fabrication of freestanding ultrathin film with thickness down to a few micrometers, as well as excellent mechanical properties and surface morphology (Figure 1e). The extremely high light transparency, ultrathin thickness, ultralight weight and easy manipulation properties of this self-healing elastomer film possess great potential in flexible electronics.

Materials characterization and self-healing ability. Figure 2a shows the aggregation of the soft segments (dark areas) and stiff segments (bright areas), which clearly exhibits a uniformly nanoscale phase separation. Upon external mechanical strain or stress, the soft segments can absorb the energy and deformation, thus exhibiting excellent stretchability. The stiff segments containing dynamic disulfide bonds are located in the soft phase matrix, and the molecular chain is fixed below T_g to maintain the mechanical toughness of the elastomer.

While keeping the amount of soft phase consistent, changing the ratio of dynamic disulfide bonds greatly influences T_g of the elastomer. As shown in Table S1, the T_g of the elastomers is able to be well tuned from 12.5 ^{o}C to 56.2 ^{o}C with the bond ratios increased from 0 to 9%. Meanwhile, the toughness of the elastomer is also increased with the amount of disulfide bonds, as a result of more stiff segments (Figure S1). The Fourier transform infrared spectra (FTIR) (Figure S2 and Table S2) and nuclear magnetic resonance (NMR) (Figure S3) are shown in the Supporting Information. The trade-off between the tensile strain limit and mechanical toughness can be further controlled through varying the ratio of the hard segments and the soft segment to fit the demands. As shown in Figure 2b and Figure 2c, the elastomer is highly stretchable, and a sample with a disulfide bond ratio of 3% is able to be stretched to 27 times the original length, which is among the best values reported[22]. To investigate the self-healing property of the elastomer, 2-mm-thick films with different ratios of disulfide bonds were fully cut through and healed at 50 ^{o}C in an oven. Repeatable self-healing tests show that the mechanical properties can be gradually recovered with the increased treating time, and 90% the mechanical strength is able to be recovered after 24 h for all the samples (Figure 2b and Figure S4). While the ratio of disulfide bonds greatly affects the initial healing rate, based on which the sample with a ratio of 8 wt% is the best and utilized for device fabrication in the following experiments. As shown in the optical microscopic images in Figure 2d, a cut on the film is visually completely healed without any trace of damage after healing at 50 ^{o}C for 5 min, indicating the fast healability of the elastomer. The interactions of disulfide content and hydrogen bonding heal individual interfaces as well as fresh wounds. The transmittances of the elastomer are nearly identical before and after healing (Figure S5). Two pieces of different elastomers were further colored in pink and blue, respectively, and treated in the same way as the previous samples. The as-healed

sample also exhibits similar elastic properties, being able to be stretched or bent (Figure 2e).

Ultrathin, transparent triboelectric skin. Among various of flexible electronic technologies, triboelectric nanogenerators (TENGs) that can convert mechanical energy into electricity based on coupling effects of contact electrification and electrostatic induction have emerged as promising energy harvesters[23-29] and self-powered active sensors[30-36]. The merits of TENGs include low cost, diverse material option, feasible fabrication, high power output at low frequencies and the ability to harvest random mechanical energy. Although the materials choices and structural designs of TENGs are quite universal to manufacture robust devices, mechanical damage is unavoidable during operation. Transparency is required in human-machine interfaces that combine sensing and displays. Multifunctional TENGs based on self-healing and transparent materials are thus highly desirable.

Figure 3a demonstrates the conformable attachment of the ultrathin triboelectric skin on a wrist. The device is composed of the self-healing elastomer as triboelectric layer and transparent conducting polymer, poly(3,4-ethylenedioxythiophene): polystyrene sulfonate (PEDOT:PSS). As shown in Figure 3b, the purchased polystyrene nanospheres with diameters of 360 nm were diluted 1:1 (in volume) with ethanol and injected slowly onto water surface to form a monolayer. The elastomer-coated substrate placed under the water in advance was lifted above the wafer surface slowly to land the polystyrene monolayer on it; afterwards the wafer was placed open to the air for water evaporation. PEDOT:PSS was further spin-coated onto the nanosphere, so that the nanosphere could be sandwiched between the elastomer and the conducting polymer to enhance

sensitivity under mechanical deformation. PEDOT:PSS of ~200 nm is applied in this structure considering the trade-off between the transmittance and conductivity (Figure S6). The as-fabricated ultrathin TENG exhibits a high average transparency of over 92% before and after healing in the visible wavelength range (400-800 nm) with a total device thickness of around 3-μm-thick (Figure 3c). The ultrathin configuration of this devices represents a reduction of thickness for more than two orders of magnitude compared with the best value achieved in previous self-healing TENGs (Table S2), which greatly improves the flexibility and reduces the total volume and weight, while maintaining a state-of-the-art transparency.

To characterize the performance of the ultrathin TENG, polytetrafluoroethylene (PTFE), one of the mostly investigated triboelectric materials with strong electron affinity, is selected as the standard contact dielectric material for reference (Figure S7). The inset of Figure 3d illustrates the device structure of a TENG in contact-separation mode, where spin-coated conductive PEDOT:PSS layer is sandwiched between the elastomers and PTFE as electrode. The device generates alternating voltage and current outputs upon contact-separation process with the coupling effects of contact electrification and electrostatic induction. Due to the strong electron affinity of PTFE, it will be negatively charged when contacting with the elastomer, as a result of charge transfer or electron injection from the later. After separation of the two materials, positive charges remain on the elastomer, inducing a layer of excessive negative charges in the PEDOT:PSS. Electrons will flow back and forth through external circuit to achieve potential equilibrium with the variation of the separation distance, resulting in an alternating current.

Typical output voltage, short-circuit current density and charge density of the ultrathin TENG were characterized in a constant contact-separation condition

controlled by a liner motor and shown in Figure 3d and Figure S8 (force, 5 N; frequency, 1 Hz; active area, 2 cm × 2 cm; separation distance, 10 cm). The device generated an open-circuited voltage of ≈26 V, a current density of ≈200 nA/cm^2 and a charge density of ≈12 nC/cm^2, demonstrating the ability as an energy harvester. The maximum peak value of the output power is 965 nW/cm^2 at an external loading of 20 MΩ (Figure S9). Such an ultrathin design greatly improves the mechanical durability of the device. It exhibits almost no performance decay after 45,000 bending cycles at a bending radius of 0.5 mm (Figure 3e). The slight difference in generated signals is caused by the different samples and setup, while the values of voltages are still consistent. This ultrathin TENG also shows extremely high operational stability, maintaining identical electrical output after 146,000 cycles' contact-separation operation conducted by a linear motor (Figure 3f and Figure S10). The excellent mechanical properties of the device are attributed to the ultrathin design as well as the intrinsic robustness of the elastomer.

Electrical outputs of the ultrathin TENG before mechanical damage and after healing are shown in Figure 3g. The film attached on a flat stage was completely cut and subsequently attached and healed for 5 min with the hot airflow from a normal hair dryer. The dynamically exchange of the disulfide bonds at the interface eventually heals the wound and connects the conductive polymer tightly, hence recovering the film conductivity. The nearly identical voltages demonstrate the fast healability of the electrical performance in device level. The resistance of the film was decreased dramatically to 2.7 × 10^9 Ω at the cut, and gradually recovered back to the original value of ~1.1 × 10^9 Ω after healing for ~5 min, which verifies the resistance recovery of the electrode (Figure S11) One of the major parameters to determine the degree of the charge density between two given

materials is the effective contact area, which is dominated by the applied force and the surface condition. Figure 3h depicts the relationship between the generated voltages and the applied forces on the TENG. The voltages of device without nanospheres quickly increase from 26.5 V to 30.8 V at first touch to 15 N force. While the nanosphere-based TENG exhibits much slower saturation rate from 14.5 V to 32.12 V, indicating the much higher sensitivity induced by the nanostructures. It can be clearly seen that both the fitting results of the voltage response could be divided into two regions based on different sensitivity in Figure 3h. For the device without nanospheres, the sensitivity in region I was 2.01 V/N, much higher than that of 0.11 V/N in region II. While for the device without nanospheres, the sensitivities in region I and II were 2.66 V/N and 0.30 V/N, respectively. The function of the nanosphere is to increase the sensitivity by creating more space during the contact-separation process. Compared to two flat surfaces, the the nanosphere-sandwiched surfaces undergo larger mechanical deformation at certain pressure before saturation, thus it can enhance the touching sensitivity[37, 38]. This voltage-force relationship makes the TENG not only an energy harvester, but also a self-powered tactile sensor. Furthermore, the electrostatic induction between two charged surfaces generates distance-dependent varying voltages. As shown in Figure 3i, the output voltage is shown to be inversely connected with the distance of the two charged objects, which is surface structure independent, differing from the contact-separation mode. This voltage-distance relationship enables the realization of a smart, non-touch and self-powered active sensor that can conformably laminated onto human skin. As a demonstration, the ultrathin triboelectric skin attached on a finger is able to actively induce voltages by approaching a piece of a paper at varying distance without contacts (Figure S12 and Video S1).

Non-contact gesture control smart system. Screens are broadly applied in daily used electronic devices as displays and human-machine interactive medium, especially for computers and smart mobile phones. Although there are screen protectors capable of self-healing scratches, no connection with the function of the mobile phone has ever been built. Herein, based on the multifunctional triboelectric skin, we develop an intelligent non-contact gesture control system on a mobile phone screen to demonstrate their potential applications in smart human-machine interaction (Figure 4). The schematic example of applications and process flow in Figure 4a summarize the overall system operation, which includes real-time signal acquisition, data processing and software decision. As human body is usually charged in daily life, a gentle wave of the hand above the ultrathin triboelectric skin that attached onto the screen can generate induced voltage signals at certain distance (Figure S13, Video S2 and Video 3). As shown in Figure 3i, the sensing voltages are subject to the distance of the approaching objects, thus decisions can be made on whether to activate the functions in the predesigned applications on the phone by setting the voltage threshold at a specific range. For the feasibility of demonstration, the ultrathin and transparent triboelectric skin is directly laminated onto a normal plastic screen protector and then attached the protector on the screen of a mobile phone, with negligible decrease of the display quality (Figure 4b). Waving hand at distances above the screen from ~1 cm to ~10 cm generates voltages from ~0.11 V to 0.08 V, respectively, which is consistent with the aforementioned results (Figure S14 and Video S4). A fully recovered signal was measured before the most common seen film scratching and after the healing with a normal electric hair drier in 2 min (Figure 4c and Video S5). A wave of hand above the smart skin at certain distance will induce a voltage captured by the external circuit, which is composed of a logic module, a data processing module, a control and collect module, and data communication module.

Once the generated voltage falls between the activation voltage threshold, the circuited will be activated and send a signal to the predesigned software application that has been installed on the smartphone as the executive program (Figure S15). After processing the induced signal, smart control of the cellphone such as answering and hanging up a phone call with noncontact gesture has been successfully achieved on both screen and human skin (Figure 4d and Figure 4e, Video S6 and Video S7). This, to our knowledge, is the first non-contact control of a smart phone with self-healing and transparent devices directly assembled on the screen and on-skin. More sophisticated non-touch control can be realized in the future through proper task assignment and region segmentation, which will be promising for convenient hand-free control and multifunctional human-device interaction.

Conclusion

In conclusion, we have developed an ultrathin self-healing triboelectric skin that exhibits excellent flexibility, high transparency, and extreme robustness. The amorphous microphase separation of the stiff segments and soft segments induced by the irregular molecular chains and strong hydrogen bonding significantly improve the transparency and mechanical properties of the elastomer. Combination of such elastomer with highly transparent and conductive polymer electrode enables the fabrication of ultrathin triboelectric device that is able to be conformably attached onto human skin for body motion energy harvesting and self-powered sensing. We demonstrate the application of such multifunctional electronic skins on a smart phone, serving as self-powered active sensor and non-touch smart control medium. This work can provide unique and robust electronics for soft robotics, human-machine interactions and flexible displays.

Supporting Information

Ratio of dynamic disulfide bonds and T_g of the elastomer, comparison of self-healing TENGs, tensile-strain of the elastomer, self-healing efficiencies of the elastomers, transmittance and sheet resistance of PEDOT:PSS film, electrical output of the TENGs, flowchart of the software design on smart phone

Acknowledgements

Research was supported by the National Key R & D Project from Minister of Science and Technology (2016YFA0202704), National Natural Science Foundation of China (Grant No. 61774016, 21774135, 5151101243, 51561145021), and Beijing Municipal Science & Technology Commission (Z171100000317001, Z171100002017017, Y3993113DF).

Author contributions

R.L. conceived the project and designed experiments. X.D., J.W. and Z.L.W. guided the project. R.L. lead the experiments, Y.L. synthesized the elastomers and S.L. performed the device test. The software was designed by F.W. in Tsinghua University. J.S. and D.L. contributed to setup and data interpretation. R.L. wrote the paper, and all the authors provided feedback.

Competing interests

The authors declare no competing interests

References

1. S. I. Rich, R. J. Wood, C. Majidi. Untethered soft robotics. Nat. Electron. 1, (2018) 102-112.
2. T. Someya, M. Amagai. Toward a new generation of smart skins. Nat. Biotechnol. 37, (2019) 382-388.
3. J. Kang, J. B.-H. Tok, Z. Bao. Self-healing soft electronics. Nat. Electron. 2, (2019) 144-150.
4. Y. Cao, Y. J. Tan, S. Li, W. W. Lee, H. Guo, Y. Cai, C. Wang, B. C.-K. Tee. Self-healing electronic skins for aquatic environments. Nat. Electron. 2, (2019) 75-82.
5. T. Someya, Z. Bao, G. G. Malliaras. The rise of plastic bioelectronics. Nature 540, (2016) 379-385.
6. T. Yokota, T. Nakamura, H. Kato, M. Mochizuki, M. Tada, M. Uchida, S. Lee, M. Koizumi, W. Yukita, A. Takimoto. A conformable imager for biometric authentication and vital sign measurement. Nat. Electron. 3, (2020) 113-121.
7. H. Jinno, K. Fukuda, X. Xu, S. Park, Y. Suzuki, M. Koizumi, T. Yokota, I. Osaka, K. Takimiya, T. Someya. Stretchable and waterproof elastomer-coated organic photovoltaics for washable electronic textile applications. Nat. Energy 2, (2017) 780-785.
8. S. Lee, D. Sasaki, D. Kim, M. Mori, T. Yokota, H. Lee, S. Park, K. Fukuda, M. Sekino, K. Matsuura, T. Shimizu, T. Someya. Ultrasoft electronics to monitor dynamically pulsing cardiomyocytes. Nat. Nanotechnol. 14, (2019) 156-160.
9. S. Lee, A. Reuveny, J. Reeder, S. Lee, H. Jin, Q. Liu, T. Yokota, T. Sekitani, T. Isoyama, Y. Abe. A transparent bending-insensitive pressure sensor. Nat. Nanotechnol. 11, (2016) 472.
10. Y. J. Tan, H. Godaba, G. Chen, S. T. M. Tan, G. Wan, G. Li, P. M. Lee, Y. Cai, S. Li, R. F. Shepherd. A transparent, self-healing and high-κ dielectric for low-field-emission stretchable optoelectronics. Nat. Mater. 19, (2020) 182-188.
11. E. J. Markvicka, M. D. Bartlett, X. Huang, C. Majidi. An autonomously electrically self-healing liquid metal–elastomer composite for robust soft-matter robotics and electronics. Nat. Mater. 17, (2018) 618-624.
12. J. Xiong, G. Thangavel, J. Wang, X. Zhou, P. S. Lee. Self-healable sticky porous elastomer for gas-solid interacted power generation. Sci. Adv. 6, (2020) eabb4246.
13. X. Yu, C. Li, C. Gao, X. Zhang, G. Zhang, D. Zhang. Incorporation of hydrogen-bonding units into polymeric semiconductors toward boosting charge mobility, intrinsic stretchability, and self-healing ability. SmartMat 2, (2021) 347-366.

14. J. Y. Oh, D. Son, T. Katsumata, Y. Lee, Y. Kim, J. Lopez, H.-C. Wu, J. Kang, J. Park, X. Gu. Stretchable self-healable semiconducting polymer film for active-matrix strain-sensing array. Sci. Adv. 5, (2019) eaav3097.
15. Y. C. Lai, H. M. Wu, H. C. Lin, C. L. Chang, H. H. Chou, Y. C. Hsiao, Y. C. Wu. Entirely, intrinsically, and autonomously self-healable, highly transparent, and superstretchable triboelectric nanogenerator for personal power sources and self-powered electronic skins. Adv. Funct. Mater. 29, (2019) 1904626.
16. D. Yang, Y. Ni, X. Kong, S. Li, X. Chen, L. Zhang, Z. L. Wang. Self-healing and elastic triboelectric nanogenerators for muscle motion monitoring and photothermal treatment. ACS Nano 15, (2021) 14653-14661.
17. K. Parida, V. Kumar, W. Jiangxin, V. Bhavanasi, R. Bendi, P. S. Lee. Highly transparent, stretchable, and self-healing ionic-skin triboelectric nanogenerators for energy harvesting and touch applications. Adv. Mater. 29, (2017) 1702181.
18. J. Deng, X. Kuang, R. Liu, W. Ding, A. C. Wang, Y. C. Lai, K. Dong, Z. Wen, Y. Wang, L. Wang. Vitrimer elastomer-based jigsaw puzzle-like healable triboelectric nanogenerator for self-powered wearable electronics. Adv. Mater. 30, (2018) 1705918.
19. Y. Lai, X. Kuang, P. Zhu, M. Huang, X. Dong, D. Wang. Colorless, transparent, robust, and fast scratch-self-healing elastomers via a phase-locked dynamic bonds design. Adv. Mater. 30, (2018) 1802556.
20. J.-A. Huang, Y.-Q. Zhao, X.-J. Zhang, L.-F. He, T.-L. Wong, Y.-S. Chui, W.-J. Zhang, S.-T. Lee. Ordered Ag/Si Nanowires Array: Wide-Range Surface-Enhanced Raman Spectroscopy for Reproducible Biomolecule Detection. Nano Lett. 13, (2013) 5039-5045.
21. R. Liu, J. Wang, T. Sun, M. Wang, C. Wu, H. Zou, T. Song, X. Zhang, S.-T. Lee, Z. L. Wang, B. Sun. Silicon Nanowire/Polymer Hybrid Solar Cell-Supercapacitor: A Self-Charging Power Unit with a Total Efficiency of 10.5%. Nano Lett. 17, (2017) 4240-4247.
22. K. Parida, G. Thangavel, G. Cai, X. Zhou, S. Park, J. Xiong, P. S. Lee. Extremely stretchable and self-healing conductor based on thermoplastic elastomer for all-three-dimensional printed triboelectric nanogenerator. Nat. Commun. 10, (2019) 2158.

23. J. Wang, S. Li, F. Yi, Y. Zi, J. Lin, X. Wang, Y. Xu, Z. L. Wang. Sustainably powering wearable electronics solely by biomechanical energy. Nat. Commun. 7, (2016) 12744.
24. J. Wang, C. Wu, Y. Dai, Z. Zhao, A. Wang, T. Zhang, Z. L. Wang. Achieving ultrahigh triboelectric charge density for efficient energy harvesting. Nat. Commun. 8, (2017) 88.
25. D. Liu, X. Yin, H. Guo, L. Zhou, X. Li, C. Zhang, J. Wang, Z. L. Wang. A constant current triboelectric nanogenerator arising from electrostatic breakdown. Sci. Adv. 5, (2019) eaav6437.
26. J. Chen, Y. Huang, N. Zhang, H. Zou, R. Liu, C. Tao, X. Fan, Z. L. Wang. Micro-cable structured textile for simultaneously harvesting solar and mechanical energy. Nat. Energy 1, (2016) 16138.
27. W. Xu, H. Zheng, Y. Liu, X. Zhou, C. Zhang, Y. Song, X. Deng, M. Leung, Z. Yang, R. X. Xu. A droplet-based electricity generator with high instantaneous power density. Nature 578, (2020) 392-396.
28. R. Hinchet, H.-J. Yoon, H. Ryu, M.-K. Kim, E.-K. Choi, D.-S. Kim, S.-W. Kim. Transcutaneous ultrasound energy harvesting using capacitive triboelectric technology. Science 365, (2019) 491-494.
29. N. Cui, C. Dai, J. Liu, L. Gu, R. Ge, T. Du, Z. Wang, Y. Qin. Increasing the output charge quantity of triboelectric nanogenerators via frequency multiplication with a multigap-structured friction layer. Energy Environ. Sci. 13, (2020) 2069-2076.
30. H. Guo, X. Pu, J. Chen, Y. Meng, M.-H. Yeh, G. Liu, Q. Tang, B. Chen, D. Liu, S. Qi. A highly sensitive, self-powered triboelectric auditory sensor for social robotics and hearing aids. Sci. Robot. 3, (2018).
31. R. Liu, X. Kuang, J. Deng, Y. C. Wang, A. C. Wang, W. Ding, Y. C. Lai, J. Chen, P. Wang, Z. Lin. Shape memory polymers for body motion energy harvesting and self-powered mechanosensing. Adv. Mater. 30, (2018) 1705195.
32. X. Peng, K. Dong, C. Ye, Y. Jiang, S. Zhai, R. Cheng, D. Liu, X. Gao, J. Wang, Z. L. Wang. A breathable, biodegradable, antibacterial, and self-powered electronic skin based on all-nanofiber triboelectric nanogenerators. Sci. Adv. 6, (2020) eaba9624.
33. X. Zhao, Z. Zhang, Q. Liao, X. Xun, F. Gao, L. Xu, Z. Kang, Y. Zhang. Self-powered user-interactive electronic skin for programmable touch operation platform. Sci. Adv. 6, (2020) eaba4294.

34. X. Pu, H. Guo, J. Chen, X. Wang, Y. Xi, C. Hu, Z. L. Wang. Eye motion triggered self-powered mechnosensational communication system using triboelectric nanogenerator. Sci. Adv. 3, (2017) e1700694.
35. X. Pu, Q. Tang, W. Chen, Z. Huang, G. Liu, Q. Zeng, J. Chen, H. Guo, L. Xin, C. Hu. Flexible triboelectric 3D touch pad with unit subdivision structure for effective XY positioning and pressure sensing. Nano Energy 76, (2020) 105047.
36. X. Pu, S. An, Q. Tang, H. Guo, C. Hu. Wearable triboelectric sensors for biomedical monitoring and human-machine interface. iScience 24, (2021) 102027.
37. K. Y. Lee, H.-J. Yoon, T. Jiang, X. Wen, W. Seung, S.-W. Kim, Z. L. Wang. Fully Packaged Self-Powered Triboelectric Pressure Sensor Using Hemispheres-Array. Adv. Energy Mater. 6, (2016) 1502566.
38. Y.-C. Lai, J. Deng, R. Liu, Y.-C. Hsiao, S. L. Zhang, W. Peng, H.-M. Wu, X. Wang, Z. L. Wang. Actively Perceiving and Responsive Soft Robots Enabled by Self-Powered, Highly Extensible, and Highly Sensitive Triboelectric Proximity- and Pressure-Sensing Skins. Adv. Mater. 30, (2018) 1801114.

Figure 1

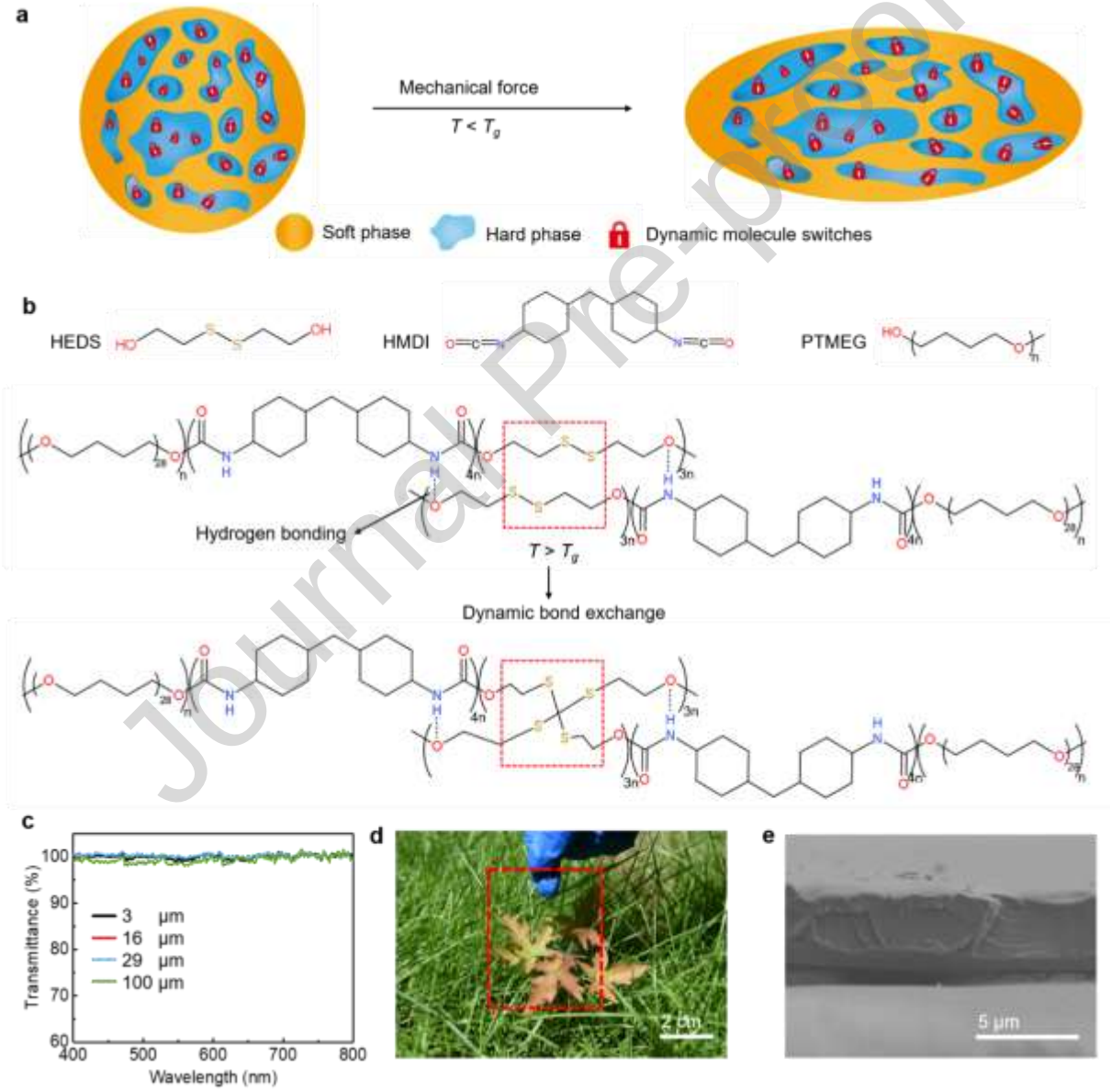

Figure 1 | Design of the highly transparent, robust and self-healing thermoplastic elastomers. a, Schematic illustration and molecular structures of the self-healing elastomers. **b,** The elastomers self-heal via dynamic disulfides and strong hydrogen bonding interactions above the glass transition temperature (T_g). **c**, Transmittance spectra of the elastomers with different film thickness. **d**, Photograph and **e**, cross-sectional scanning electron microscopy (SEM) image of a 3-μm-thick elastomer film.

Figure 2

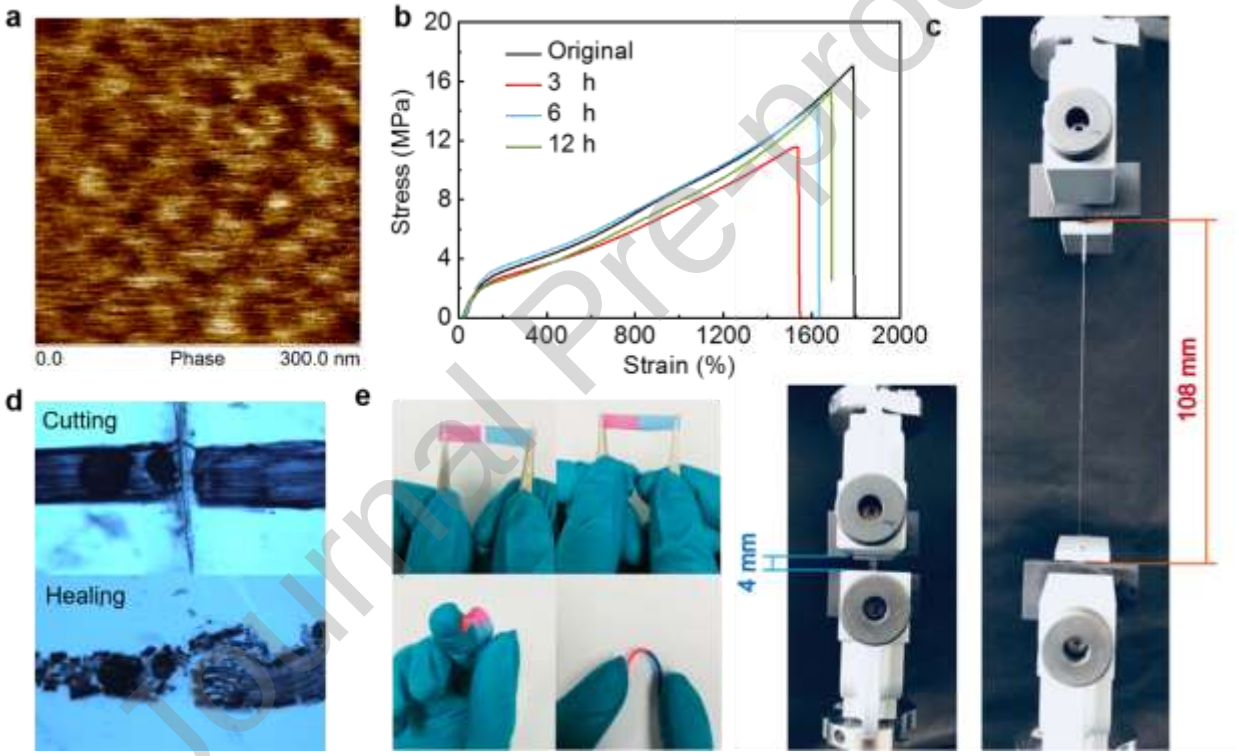

Figure 2 | Characterization and healing behaviors. a, Atomic force microscopy (AFM) images of the elastomers. **b**, Strain-stress curves of the elastomers with a disulfide bond ratio of 8% before cut and after healing for varying time at 50 ^{o}C. **c**, Photographs of the elastomer with a disulfide bond ratio of 3% being stretched at 0% and 2600% strain. **d**, Optical images of a 2-mm-thick elastomer before cutting (top) and after healing (bottom) at 50 ^{o}C for 5 min. The top of the film is marked by ink. **e**, Photographs of two different pieces of elastomers colored in pink and blue being stretched and bent after healing.

Figure 3

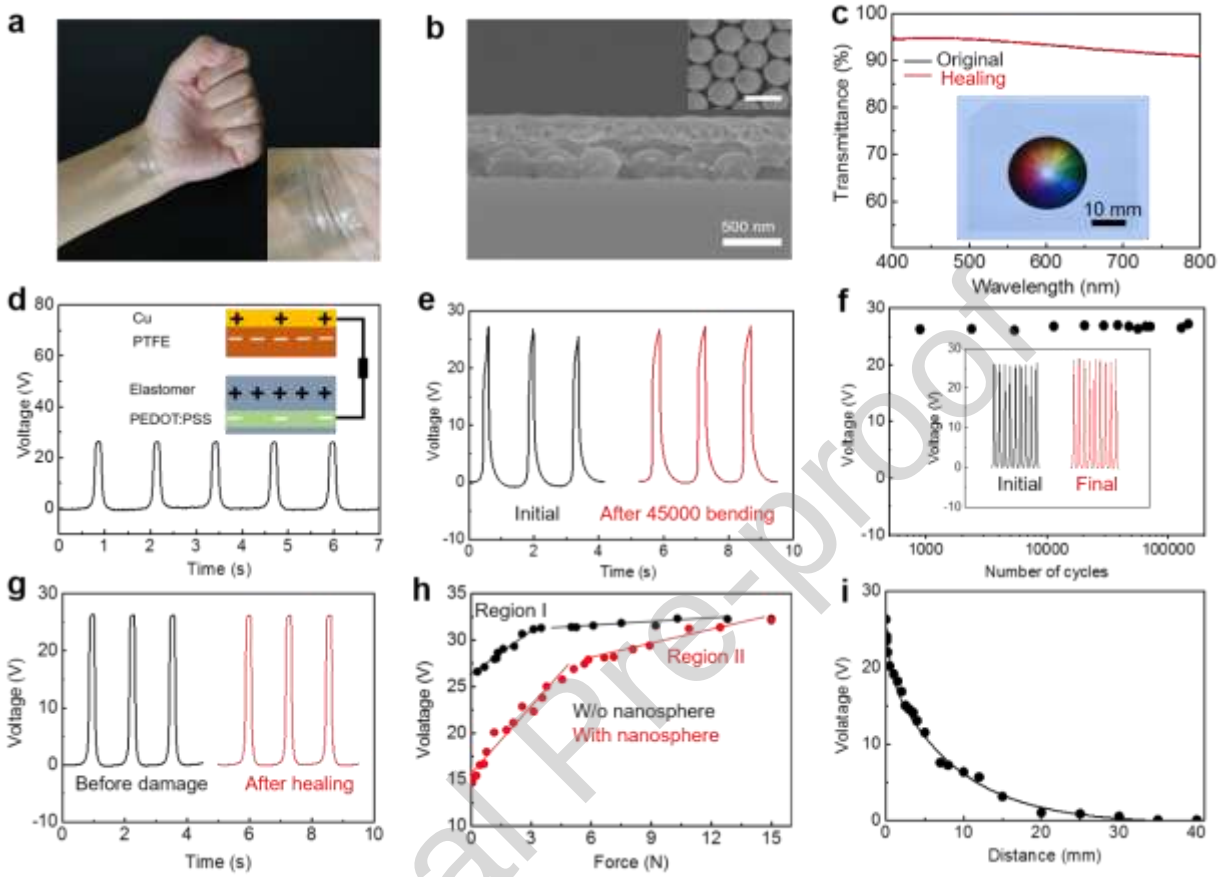

Figure 3 | Design, optical and electrical characteristics of the ultrathin, highly transparent and self-healing triboelectric nanogenerators (TENGs). a, Photograph of the triboelectric skin attached on a wrist. Inset is a magnified image of the device perfectly fitted onto the wrinkles of the wrist. **b**, Cross-sectional SEM image of the ultrathin TENG with polystyrene nanospheres (diameter, 360 nm) embed between elastomer layer and PEDOT:PSS to enhance the tactile sensitivity. Inset is a SEM image of the nanosphere without covering. Scale bar: 500 nm. **c**, Transmittance spectra of a 3-μm-thick TENG before and after healing. An average transmittance over 92% is recorded in the visible range (400-800 nm). Inset is a photograph of the device on a printed color panel. **d**, Voltage of the TENG working in a contact-separation mode with PTFE/Cu, driven by a linear motor (area: 4 cm^2; frequency: 1 Hz; force: 5 N). Inset is schematic diagram and working principle of the TENG, where self-healing elastomer is used as the triboelectric layer and PEDOT:PSS is used as the current collector. **e**. Bending results of the TENG at a radius of 0.5 mm. **f**, Operational stability test of the TENG during over

146,000 cycles. **g**, The output voltages of the TENG before mechanical damage and after healing. **h**, The influence of the mechanical force on the output voltages of the TENGs with and without nanosphere. **i**, Generated voltages to the separation distance, as a result of electrostatic induction.

Figure 4

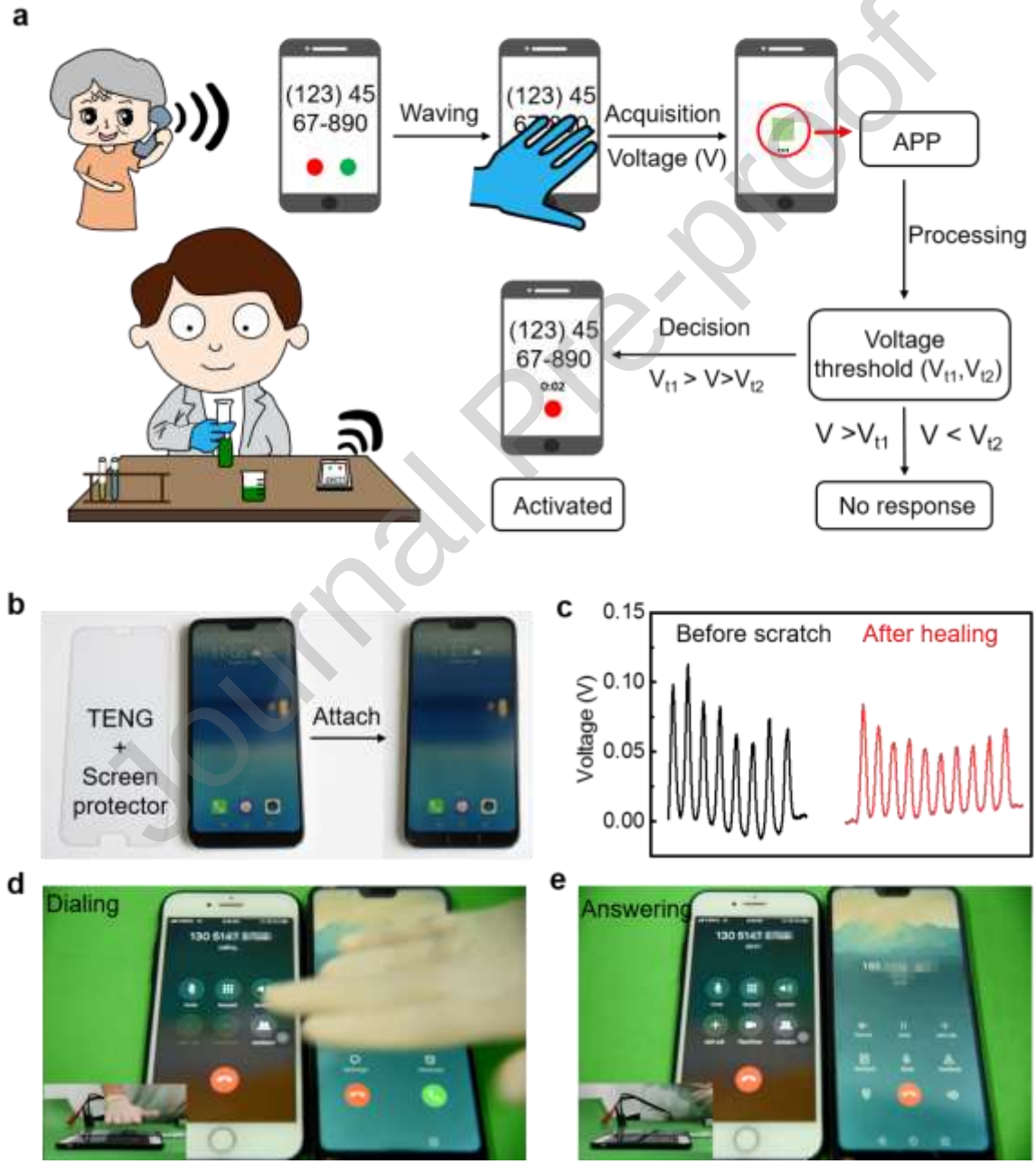

Figure 4 | Non-contact gesture control application. a, Schematic drawing and process flow of the non-touch gesture control system. **b**, Photographs of the ultrathin TENG on a screen protector before and after attached onto a mobile phone. **c**, Induced voltage signals from the screen the before scratch and after healing, by waving hand with glove above the screen at a distance of ~2 cm. **d**, Waving hand above the screen at a phone call and **e**, answering the phone call after the waving.

Table of Contents

An ultrathin, highly transparent and robust self-healing e-skin for self-powered tactile and non-contact sensing based on elastomers and conducting polymers has been developed.

CRediT authorship contribution statement

R.L. conceived the project and designed experiments. X.D., J.W. and Z.L.W. guided the project. R.L. lead the experiments, Y.L. synthesized the elastomers and S.L. performed the device test. The software was designed by F.W. in Tsinghua University. J.S. and D.L. contributed to setup and data interpretation. R.L. wrote the paper, and all the authors provided feedback.

Declaration of Competing Interest

☒ The authors declare that they have no known competing financial interests or personal relationships that could have appeared to influence the work reported in this paper.

☐The authors declare the following financial interests/personal relationships which may be considered as potential competing interests:

Highlights

- Homogeneous control of an amorphous elastomer by locking soft dynamic bonds in stiff polymer matrix enables fast self-healing materials with nearly 100% transparency and excellent mechanical properties.
- The 3-μm-thick self-healing e-skin is highly flexible and extremely robust, which can be easily conformed onto the

curvature of human skins and maintain the identical electrical output performance after 45, 000 bending tests at a radius of 0.5 mm and over 146, 000 operational cycles.

- A conformable triboelectric device based on the e-skin can generate voltages of up to 26 V with human body motion through coupling effect of contact electrification and electrostatic induction, which can be used for bioenergy harvesting and self-powered sensing.
- For the first time, we demonstrate the non-contact gesture control of a smart phone with the self-healing, transparent and self-powered e-skin, providing a new prospect for smart human-machine interactions.